ELSEVIER

Geomorphology 16 (1996) 103–119

GEOMORPHOLOGY

Quantitative topographic method of fault morphology recognition

Igor V. Florinsky [1]

Institute of Mathematical Problems of Biology, Russian Academy of Sciences, Pushchino, Moscow Region, 142292, Russia

Received 12 January 1995; revised 10 August 1995; accepted 3 September 1995

Abstract

A quantitative method for morphology recognition of topographically expressed faults is developed. The method is based on the analysis of digital elevation models (DEMs). Lineaments revealed on horizontal landsurface curvature map indicate faults formed mostly by horizontal tectonic motion (i.e., strike-slip faults). Lineaments recognized by vertical landsurface curvature mapping correspond to faults formed mainly by vertical motion (i.e., dip-slip and reverse faults) and thrusting. Lineaments recorded on both horizontal and vertical curvatures maps indicate, as a rule, oblique-slip and gaping faults.

The method is tested by processing the DEMs of an imaginary area with modeled faults and a DEM of a part of the Crimean Peninsula and the adjacent sea bottom. For the imaginary area the results obtained mostly correlate with the theoretical basis of the method. For the real area a comparative analysis of the results obtained and factual geological data demonstrate that the method actually works to identify individual faults in regions where both topography and tectonic structure are complicated.

Some aspects of the method precision, requirements for initial data and further development of the method are discussed.

1. Introduction

Faults can be revealed by several geological, geophysical, remote sensing and topographical techniques (Slemmons and Depolo, 1986). As tectonic motion can result in linear deformation of the landsurface so topographically expressed lineaments are often used as fault indicators (Hobbs, 1904; Peive, 1956; Phylosophov, 1960; Ollier, 1981). Properties of linear relief dislocations formed by vertical tectonic motions differ from properties of topographic lineaments which are horizontal movement traces (Trifonov, 1983; Keller, 1986). Qualitative and quantitative signs of these differences can be used as a basis for fault morphology recognition.

Qualitative approaches to revealing and morphological classification of faults by a relief analysis were often exploited (see reviews in Trifonov, 1983; Slemmons and Depolo, 1986). Of frequent use was a visual analysis of topographic map contours (Hobbs, 1904; Phylosophov, 1960; Nezametdinova, 1970) and remotely sensed images (Wilson, 1941; Lattman, 1958; Vinogradova and Yeremin, 1971; Trifonov et al., 1983). Keller (1986) summed up data on qualitative geomorphic indices of active faults. Stereophotogrammetric analytical techniques were applied for revealing faults, morphological recognition, dip and strike measurement (Vinogradova and Yeremin, 1971).

Indicated qualitative approaches are not free of

[1] Tel.: (7 0967) 73-08-00, (7 095) 923-35-58, Fax: (7 0967 73-24-08, E-mail: flor@impb.serpukhov.su

SSDI 0169-555X(95)00136-0

subjectivity. So tectonic quantitative geomorphology is one of the main research priorities in the field of active tectonics (Wallace, 1986). However, due to difficulties in formalization of fault geomorphic indices there are a lot of quantitative computer methods for fault revealing by remotely sensed (Burdick and Speirer, 1980; Zlatopolsky, 1988; Masuoka et al., 1988) and topographic data processing, but there is no quantitative method for fault morphological classification by outlined data handling without ancillary geological information.

Digital elevation models (DEMs) and DEM analysis methods are used for fault recognition as about 90% of fault geomorphic indices can be defined quantitatively (Schowengerdt and Glass, 1983). There are techniques of perspective views (Campagna and Levandowski, 1991; Morris, 1991), thalweg revealing (Eliason and Eliason, 1987; Thienssen et al., 1994), landsurface gradient and aspect mapping (Onorati et al., 1992). DEMs are applied for measuring dip and strike of known faults (Chorowicz et al., 1991; Morris, 1991). Of major use for fault revealing is the reflectance mapping (Wise, 1969; Schowengerdt and Glass, 1983; Moor and Simpson, 1983; Onorati et al., 1987, 1992; Morris, 1991). The comparative analysis of reflectance maps, Landsat and side-look aperture radar images has shown that reflectance mapping is preferable for fault recognition (Schowengerdt and Glass, 1983). About 90% of faults and folds recognized by geological and geophysical techniques can be revealed on reflectance maps (Onorati et al., 1992). However, the use of indicated methods of DEM analysis without ancillary geological data does not permit us to determine a fault morphology.

Reproducible recognition of lineaments can also be obtained by calculation and mapping of the horizontal (K_h) and vertical (K_v) landsurface curvatures with the use of DEMs (Florinsky, 1992). Statistical properties of lineaments (i.e., orientation, length, density) recorded on K_h maps are rather different

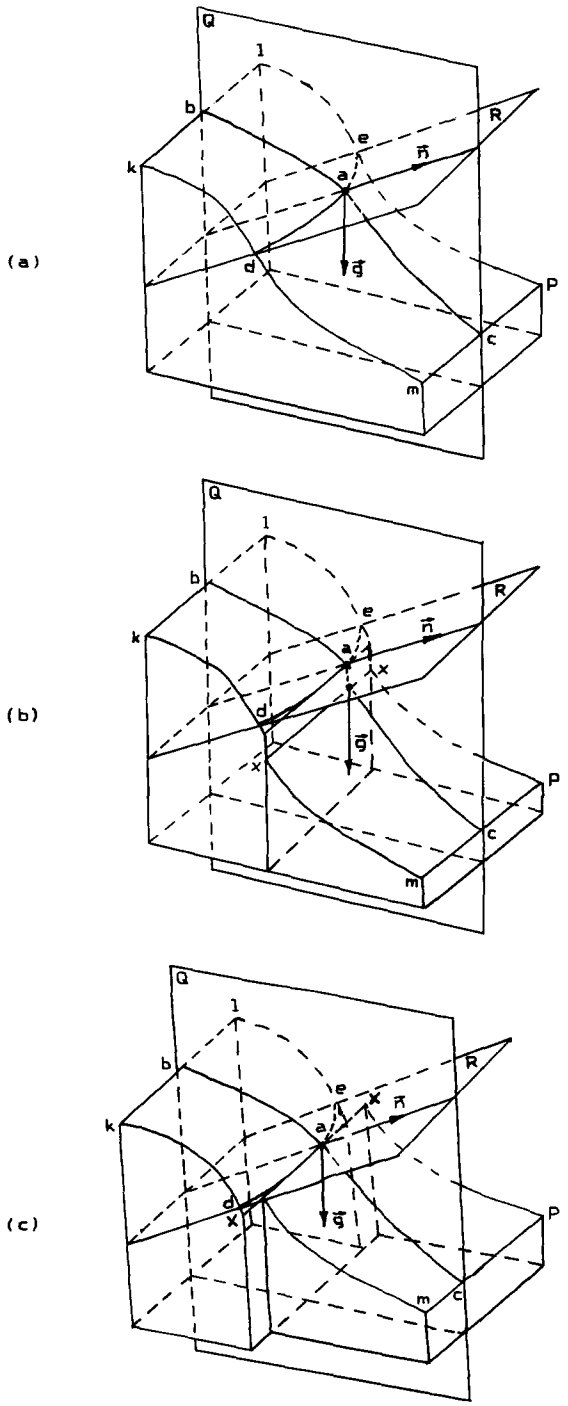

Fig. 1. Block-diagrams illustrating K_h and K_v sign changes after vertical and horizontal tectonic motions: (a) the idealized surface *klmp*, *Q* is the vertical plane which includes the normal vector *n* and the gravity acceleration vector *g* in the given point *a*, *bac* is the intersection curve of the surface *klmp* and the plane *Q*, *R* is the plane which is normal to the surface *klmp* and the plane *Q*, *dae* is the intersection curve of the surface *klmp* and the plane *R*; (b) the surface *klmp* after a dip-slip fault; (c) the surface *klmp* after a strike-slip fault, $x-x$ are fault lines.

from statistical properties of linear structures revealed by K_v mapping (Florinsky, 1992). From a geomorphological point of view, this is due to the fact that K_h mapping reveals predominantly valley and watershed spurs, while K_v mapping reveals mainly terraces (Evans, 1980). This is an automated separation of different relief elements. Taking into account physical and mathematical senses of K_h and K_v (Young, 1972; Evans, 1980; Shary, 1991) we can reason that lineaments revealed by K_h mapping correspond mostly to structures like strike-slip faults, while lineaments revealed by K_v mapping indicate mainly structures as dip-slip faults and thrusts.

In the present paper the quantitative method of morphology recognition of topographically expressed faults is suggested. The method is based on K_h and K_v calculation and mapping.

2. Theoretical basis of the method

Let us consider a surface *klmp* (Fig. 1a). K_v is the curvature of a normal section *bac* of the surface *klmp*. The section *bac* includes a gravity acceleration vector g and a normal vector n in a given point a. K_h is the curvature of a normal section *dae* of the surface *klmp*. The section *dae* is perpendicular to the section *bac* and includes the normal vector n in the given point a. K_h and K_v can be determined in any point of the surface *klmp*. If indicated sections are convex K_h and K_v have positive values, if sections are concave these curvatures have negative values, if sections are plane K_h and K_v have zero values (Young, 1972; Evans, 1980; Shary, 1991).

Suppose a dip-slip (or reverse) fault is formed within the surface *klmp* (Fig. 1b), K_h and K_v values within the scarp zone will change and besides K_v will have negative values all along a fault line x–x. Let us stratificate K_h and K_v values into two levels with respect to the zero value and paint areas with K_h and K_v positive values in white colour, while areas with negative values of curvatures are painted black. An indicator of the dip-slip (or reverse) fault that is a black lineament on a white background will be recorded on the K_v map. A similar lineament will be recognized on the K_v map if before a vertical motion a surface was plane. If before vertical motion K_v values were negative the K_v sign will also change along the fault line. Therefore a white lineament on a black background on the K_v map will indicate a dip-slip fault. A lineament consisting of black and white lines and spots will be recorded on the K_v map after a vertical movement if a surface has a complicated form. In a like manner, a lineament indicating a thrust will be revealed on the K_v map since thrusting also brings into existence a scarp, as a rule.

However, lineaments indicating dip-slip, reverse and thrust faults will not be recorded on the K_h map because changes of the K_h sign along lines of these faults will be random rather than systematic. At the same time, some non-lineament changes on the K_h map will arise.

Suppose a strike-slip fault is formed within the surface *klmp* (Fig. 1c). K_h and K_v values will also change in the deformation zone. The K_h will take negative values along all the fault line x–x, while changes of the K_v sign will be random rather than systematic. Consequently, the following lineaments indicating horizontal movement traces will be recorded on the K_h map: (a) a black lineament on a white background for the given case (Fig. 1c) and for a plane surface, (b) a white lineament on a black background for a surface with negative K_h values, and (c) a lineament consisting of white and black lines and spots for a complex surface. Some non-lineament traces of horizontal movements will be recorded on the K_v map.

After an oblique-slip and gaping fault formation both the curvatures ought to change sign systematically along lines of these structures. Therefore, we can anticipate that lineaments indicating these faults will be recorded on both the maps.

The method proposed has the following limitations:

1. It is impossible to determine and separate lineaments of non-tectonic (i.e., erosion, eolian) origin without ancillary geological, geophysical and geomorphic data.
2. Lineaments recorded on K_h and K_v maps can be connected with flexures and folds. To determine and separate these lineaments ancillary non-topographic data have to be used too.
3. If a strike-slip fault is located along a surface strike a lineament indicating this fault cannot be recorded by K_h mapping.

4. We also have to use ancillary geological data to separate: (a) a dip-slip, reverse and thrust faults equally revealed on K_v maps, and (b) an oblique-slip and gaping faults equally revealed on both K_h and K_v maps.
5. The method allows us to recognize neotectonic faults and reactivated ancient ones.

3. The method precision and requirements to initial data

K_h and K_v digital models are obtained by DEM processing which includes measuring the second and first derivatives of elevations. For example, this procedure can be realized by the algorithm of Evans (1980).

As far as we know, a precision of K_h and K_v calculation has not been properly studied so far. At the same time, the precision of gradient and aspect calculations (which include measuring only the first elevation derivatives) is often discussed (Isaacson and Ripple, 1990; Carter, 1992). Shary (1991) supposed that the K_h and K_v calculation precision cannot be determined at all. Really, a measuring precision can be defined as a difference between a measured value and a real value of a certain variable. However, the real landsurface is not mathematically smooth. Therefore, it cannot have derivatives and curvatures. These variables are abstract and arise only in the course of measuring. As there are no real values of K_h and K_v their calculation precision cannot be determined.

The cited opinion is controversial. However, the K_h and K_v calculation precision is a subject of an individual investigation. At the same time, it is obvious, that the quality of K_h and K_v calculation depends on the quality of initial data that are DEMs.

To reveal topographically expressed faults within a certain scale range initial data should meet the following main requirements:

1. A DEM has to be compiled by regular net.
2. A DEM resolution has to correspond to a typical plan size of faults under study.
3. A DEM precision has to permit "feeling" of fault traces.

Let us consider these requirements in detail (Florinsky, 1993).

1. Compilation of a sufficiently precise DEM can be realized by (a) a random irregular net, (b) an irregular net with consideration of watersheds, thalwegs, edges, foots, and (c) a random regular (i.e., square, rectangular) net (Schut, 1976; Carter, 1988). However, different typical fault sizes will correspond to different matrix steps of an irregular DEM. It can result in simultaneous revealing of faults belonging to different scale ranges on one and the same map of a given scale. So neighboring parts of this map will have different resolutions. It is also desirable to use rectangular nets because a DEM will have different resolutions along X and Y axes of the Cartesian coordinate system. Hence we have to use DEMs compiled by a square net.

Because of some technical difficulties in realization of this requirement a user often has to employ an irregular DEM as initial data. Various interpolation algorithms can be applied to generate a regular DEM from an irregular one (Schut, 1976). However, all these methods have one or another drawback. There are no impartial criteria for an estimation of the relief reconstruction precision (Schut, 1976). Artifacts could arise due to the Gibbs phenomenon (Ulyanov, 1977).

2. A typical plan size S of faults under study ought to be chosen by the user during the problem formulation. S will determine a matrix step w of a regular DEM and hence a DEM resolution. The latter ought to conform with the resulting scale of K_h and K_v maps. Otherwise the user may obtain unreadable maps.

A DEM compilation is a discretization of the landsurface elevation continuous function with respect to two variables. In accordance with the Kotelnikov theorem a one-variable continuous function with a finite spectrum (a limiting frequency is F) is uniquely determined by its values with $1/(2F)$ step (Korn and Korn, 1968). A discreting step of a two-variable function must be equal to a half period of a space harmonic corresponding to the smallest surface details (Pratt, 1978). In practice, we have to insert a reserve multiplicative coefficient 2–5 into a measured value of a limiting frequency. Suppose a size of the smallest surface detail S with space frequencies $F_x = F_y = 1/S$. Consequently, $w = S/n$, where $n = 2–5$.

3. The item of a DEM precision as applied to the

method developed is fairly complicated. On the one hand, it is obvious that a DEM ought to have rather a high precision to "feeling" fault traces. Moreover, such a precision may be unrealistic. On the other hand, utilization of DEMs with usual precision allows us to recognize the most of topographically expressed faults (Florinsky, 1992). This can be connected with an erosion influence which may increase topographic expression of faults, for instance, in forms of fault-line valleys, gaps or scarps. Now we cannot offer a quantitative criterion for a preliminary estimation of whether a DEM precision is good for fault revealing and morphological classification. This item is to be investigated. Some general reasons are given below.

There are three main approaches to a DEM compilation: topographic surveys, stereoplotter techniques and digitizing of topographic map contours (Carter, 1988). From a DEM precision point of view, it is worthwhile to use a topographic survey at a local level. It is expedient to apply stereoplotter techniques at a regional level. Contour digitizing is not good at either scale. There are random errors of contour interpolation and generalization. On occasion a contour interval cannot provide an elevation data completeness and precision which are necessary for fault recognition.

The space frequency spectrum of the landsurface is unlikely to be finite. Consequently, the Kotelnikov theorem condition (see above) is not met. However, as a rule, the user is interested in faults with S not smaller than a certain threshold. Therefore, we can consider that all the space harmonics with frequencies more than $1/S$ are noise. A DEM can also include a high frequency noise which is caused by minor errors during a DEM compilation.

It is obvious, we must decrease the noise in a DEM. Otherwise artifacts and unreadable K_h and K_v maps may be obtained. Noise decreasing can be realized by well-known methods of a surface low-pass filtering or smoothing (Bassett, 1972; Pratt, 1978). The algorithm of Evans (1980) using for K_v and K_h calculation also results in a slight elevation smoothing and a noise filtering.

During a certain displacement of a net we can compile different DEMs for one and the same area. However, a matrix step $w = S/n$ permits us to believe that a DEM includes information on all the topographically expressed faults with typical size S. So possible differences of such DEMs can be ignored.

Probably, fractal dimension (Mandelbrot, 1967) can influence K_h and K_v (Klinkenberg, 1992). However, topographic fractal models (Clarke, 1988) are not discussed here. We believe that topographically expressed faults are scale-dependent structures (Clarke, 1988). Therefore, a fractal component of topography can be considered as a noise.

4. Method testing

To test the method developed we used the DEMs of an imaginary area with modeled faults and a DEM of a part of the Crimean Peninsula and the adjacent sea bottom.

4.1. The imaginary area

4.1.1. Study site

The imaginary area (Fig. 2a) has a size of 60 m × 60 m. It includes a single near-east oriented valley and two adjacent watersheds. Elevation amplitude is 7.5 m.

4.1.2. Initial data and methods

The irregular DEM of the imaginary area including 129 points was compiled (Fig. 2a). The following seven simple typical kinds of faults (Gzovsky, 1954) were modeled by deformation of the initial irregular DEM: a vertical dip-slip fault with 1 m displacement (Fig. 2d), a low-angle dip-slip fault with 1 m displacement and 30° dip (Fig. 2g), a left-lateral strike-slip fault with 3.5 m displacement (Fig. 2j), an oblique-slip fault with 3.5 m left-lateral horizontal and 1 m vertical displacement (Fig. 2m), an overthrust with 5 m displacement (Fig. 2p), an overthrust with 15 m displacement (Fig. 2s), a gaping fault with a trench of 1 m width and 0.2 m depth (Fig. 2v). Seven irregular DEMs with indicated modeled faults were obtained.

Eight regular DEMs of initial and deformed surfaces were generated by the Delaunay triangulation and piecewise polynomial smooth interpolation (Schut, 1976) of corresponding irregular DEMs. A matrix step of 2 m was used. K_h and K_v digital

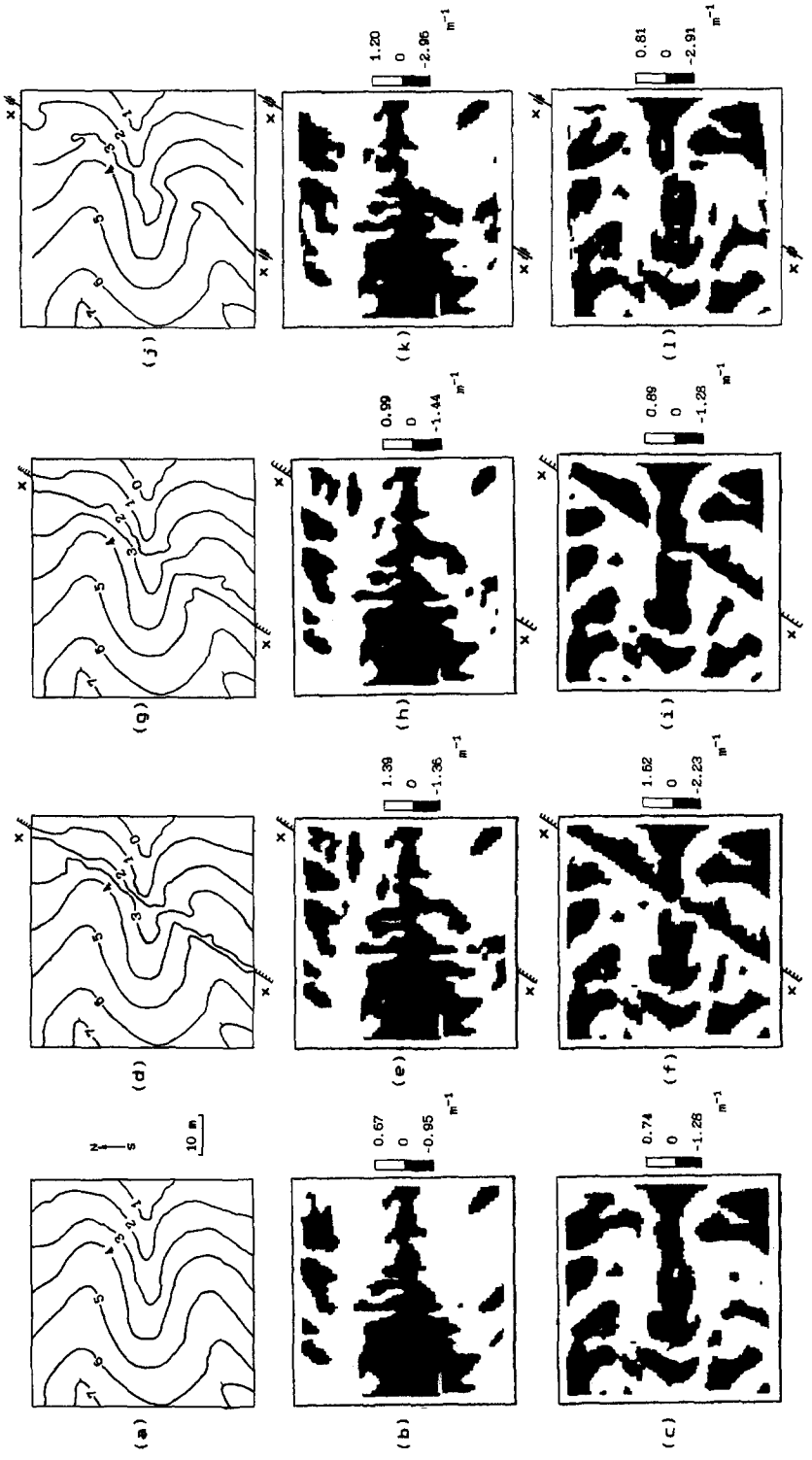
(a)
(b)
(c)
(d)
(e)
(f)
(g)
(h)
(i)
(j)
(k)
(l)
N
S
10 m
0.67
0
-0.95
0.74
0
-1.28
1.38
0
-1.36
1.62
0
-2.23
0.99
0
-1.44
0.89
0
-1.28
1.20
0
-2.96
0.81
0
-2.91
m⁻¹

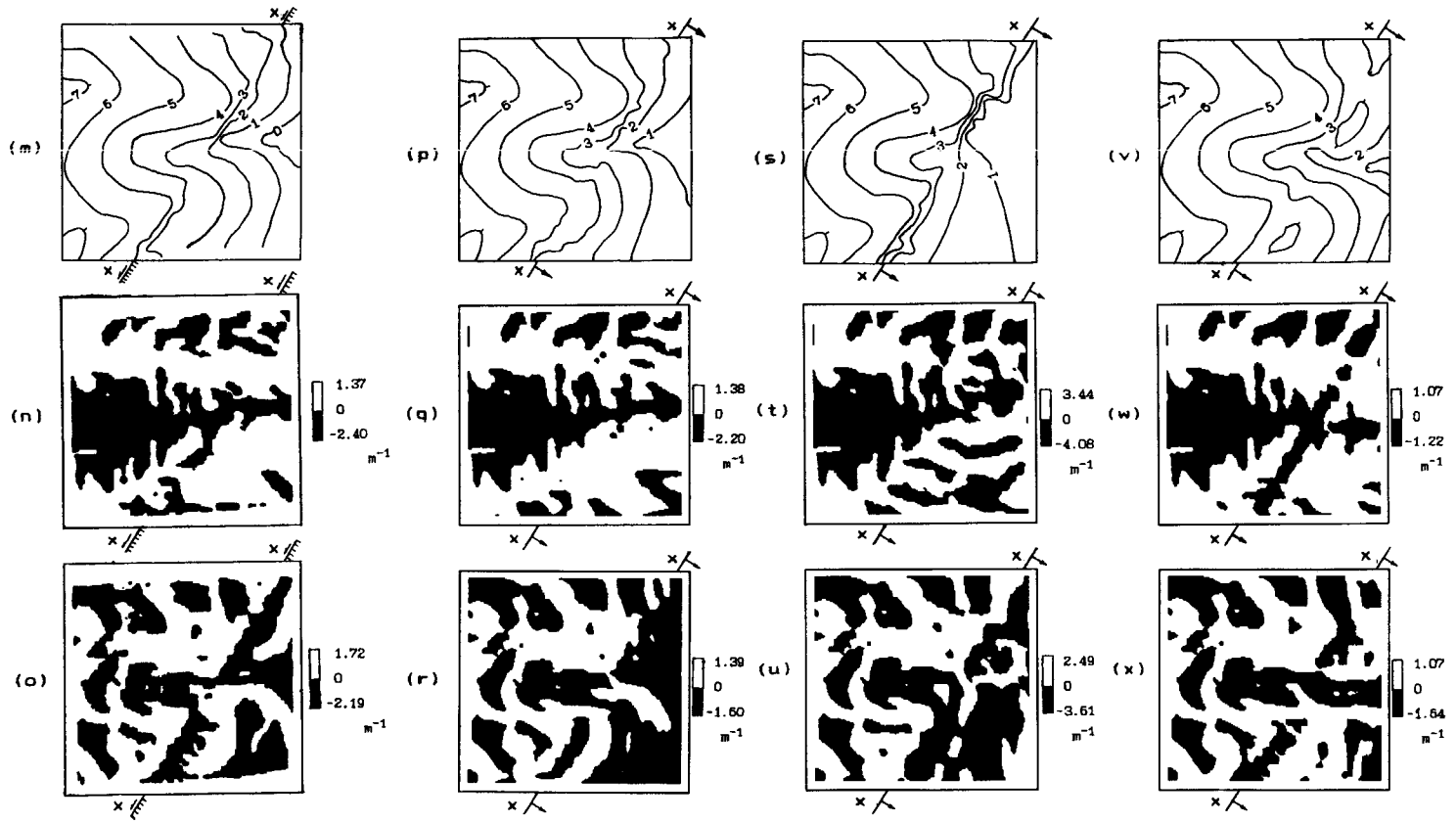

Fig. 2. Maps of the imaginary area with modeled faults, $x-x$ are fault axes: (a) the elevation of the undeformed area, (b) the K_h of the undeformed area, (c) the K_v of the undeformed area, (d) the elevation of the area with the vertical dip-slip fault, (e) the K_h of the area with the vertical dip-slip fault, (f) the K_v of the area with the vertical dip-slip fault, (g) the elevation of the area with the low-angle dip-slip fault, (h) the K_h of the area with the low-angle dip-slip fault, (i) the K_v of the area with the low-angle dip-slip fault, (j) the elevation of the area with the strike-slip fault, (k) the K_h of the area with the strike-slip fault, (l) the K_v of the area with the strike-slip fault, (m) the elevation of the area with the oblique-slip fault, (n) the K_h of the area with the oblique-slip fault, (o) the K_v of the area with the oblique-slip fault, (p) the elevation of the area with the overthrust, 5 m displacement, (q) the K_h of the area with the overthrust, 5 m displacement, (r) the K_v of the area with the overthrust, 5 m displacement, (s) the elevation of the area with the overthrust, 15 m displacement, (t) the K_h of the area with the overthrust, 15 m displacement, (u) the K_v of the area with the overthrust, 15 m displacement, (v) the elevation of the area with the gaping fault, (w) the K_h of the area with the gaping fault, (x) the K_v of the area with the gaping fault.

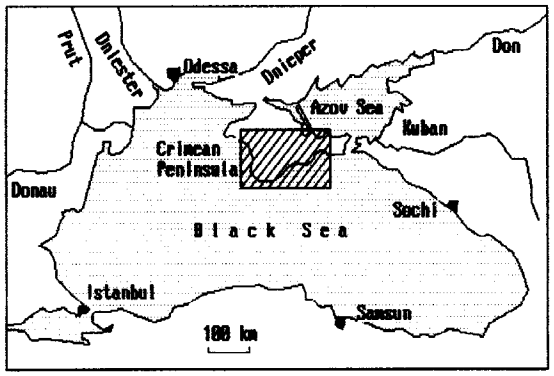

Fig. 3. Geographical location of the study site (between 44°21′ and 45°30′N and 33°13′ and 35°55′E, hachured).

models (Fig. 2b, c, e, f, h, i, k, l, n, o, q, r, t, u, w, x) for each regular DEM were calculated by the algorithm of Evans (1980).

All modeled faults have a random 28° strike. It was chosen to avoid a mathematically non-proved but widespread speculation that K_h and K_v are anisotropic operators, "feel" a square net of a DEM and are able to reveal only north, west, northwest and northeast oriented lineaments (A.M. Berlyant, pers. commun., 1991).

4.2. The part of the Crimean Peninsula and the adjacent sea bottom

4.2.1. Study site

The study site (Fig. 3) forms a part of the Crimean Peninsula and the adjacent sea bottom and has a size of 204 km × 132 km. We choose this region to test the method developed for two reasons. First, it is one of the best studied areas in the world (Muratov, 1969; Beloussov and Volvovsky, 1989). Although the geological structure of the study site is very complicated and several regional geological theories exist there are a lot of factual geological, geophysical and remotely sensed data to test fault revealing and morphology recognition. Second, a diversity of relief (Fig. 4a) and tectonic structures (Fig. 4b) within the region allow us to test the method in different topographic and geological conditions.

4.2.2. Relief description

The following main relief elements are situated within the study site: the Mountain and the Plane Crimea, the Azov Sea shallow, the Black Sea shelf, continental slope and floor (Muratov, 1969; Beloussov and Volvovsky, 1989). Elevation amplitude is 3645 m (Fig. 4a).

The Mountain Crimea stretches along the Black Sea. This territory includes three principal near-parallel ridges, two strike valleys and the South Coast of the Crimea. The highest (Main) ridge consists of the chain of table massifs with steep south slopes (elevations are 1000–1545 m) and the system of ranges (elevations are 300–1100 m). Two cuesta ridges with steep south slopes are situated north of the Main Ridge (elevations are 200–600 m). The second ridge includes some degraded mountains. The South Coast of the Crimea stretches between the Main Ridge and the Black Sea. Landslides, rockfall slopes and gullies are widespread there.

North of the Mountain Crimea there is the Plane Crimea. It is a gently sloping area with 50–150 m elevations in its central part and 0–50 m ones in its western and eastern parts. There is a peneplain between the Black Sea and the Azov Sea (elevations 80–150 m). On the northwest of the study site there is a rolling dissected plain (elevations 50–170 m).

The Azov Sea shallow is an almost flat area with 0–8 m depths. In the western and the eastern parts of the region the Black Sea shelf (depths 0–200 m) includes two broad zones adjoined to the Plane Crimea. A narrow long shelf zone stretches along the Mountain Crimea. The continental slope (depths 200–1800 m) includes some submarine ridges and is dissected by submarine valleys. Valleys stretch up to the Black Sea floor (depths 1900–2100 m) which is an extremely flat area.

Fig. 4. The part of the Crimean Peninsula and the adjacent sea bottom: (a) the elevation map obtained by the DEM processing (Florinsky, 1992), (b) the generalized tectonic scheme (Muratov, 1969; Beloussov and Volvovsky, 1989); (c) the summary scheme of main faults compiled by some published geological data (Lebedev and Orovetsky, 1966; Shalimov, 1966; Muratov, 1969; Rozanov, 1970; Lvova, 1972; Sollogub and Sollogub, 1977; Sidorenko, 1980; Kats et al., 1981; Abashin et al., 1982; Kozlovsky, 1984; Borisenko, 1986; Zaritsky, 1989), *1–1* is the Korsak–Feodosia fault, *2–2* is the Simferopol–Alushta fault, *3–3* is the South Coast fault.

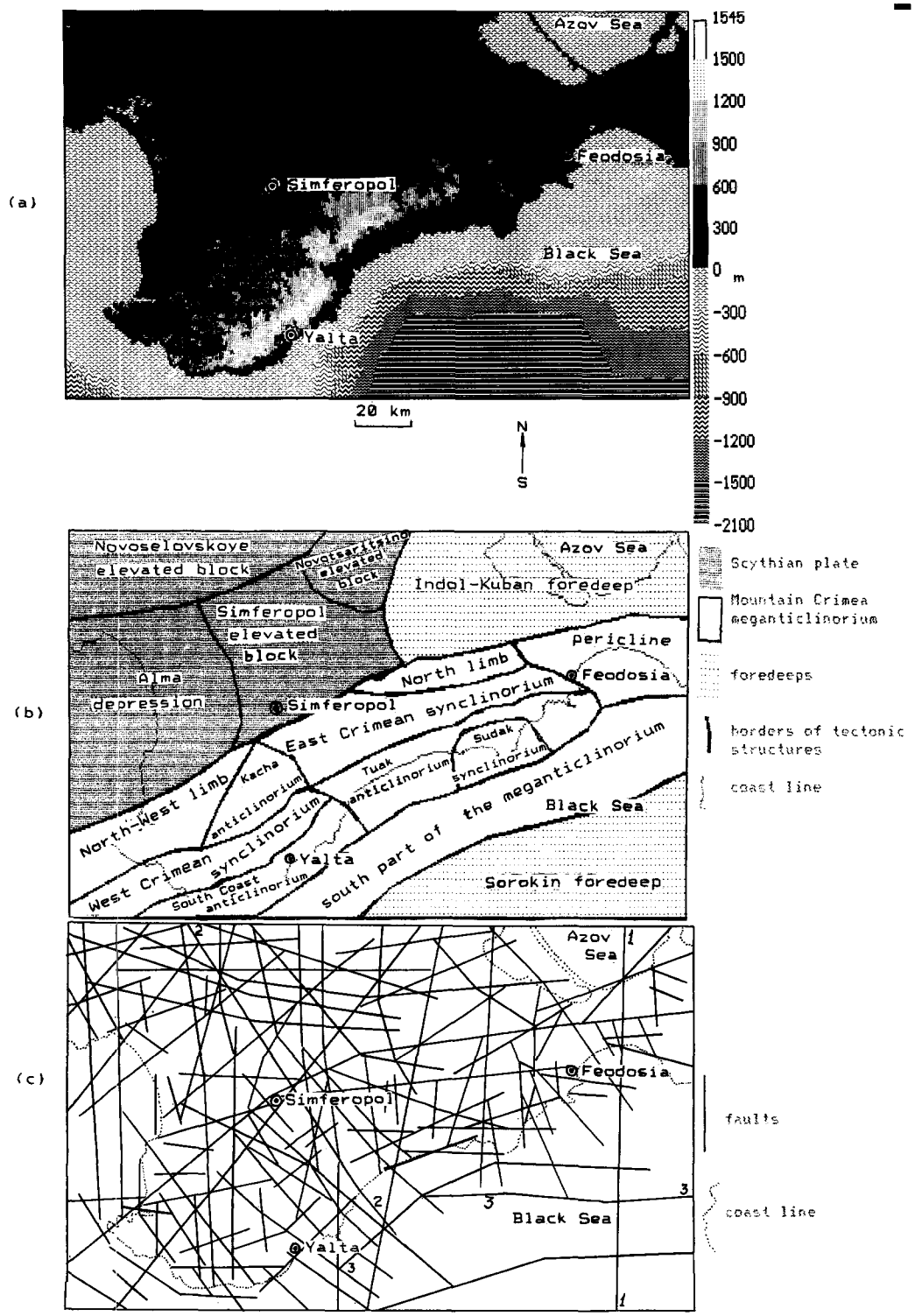
(a)
Azov Sea
Feodosia
Simferopol
Black Sea
Yalta
20 km
N
S
1545
1500
1200
900
600
300
0 m
-300
-600
-900
-1200
-1500
-2100
(b)
Novoselovskoye elevated block
Novoteritsino elevated block
Azov Sea
Indol-Kuban foredeep
Simferopol elevated block
pericline
North limb
Feodosia
Alma depression
Simferopol
East Crimean synclinorium
Sudak synclinorium
Tuak anticlinorium
Kacha anticlinorium
North-West limb
West Crimean synclinorium
South Coast antiflinorium
Yalta
south part of the meganticlinorium
Black Sea
Sorokin foredeep
Scythian plate
Mountain Crimea meganticlinorium
foredeeps
borders of tectonic structures
coast line
(c)
Azov Sea
Feodosia
Simferopol
Black Sea
Yalta
faults
coast line

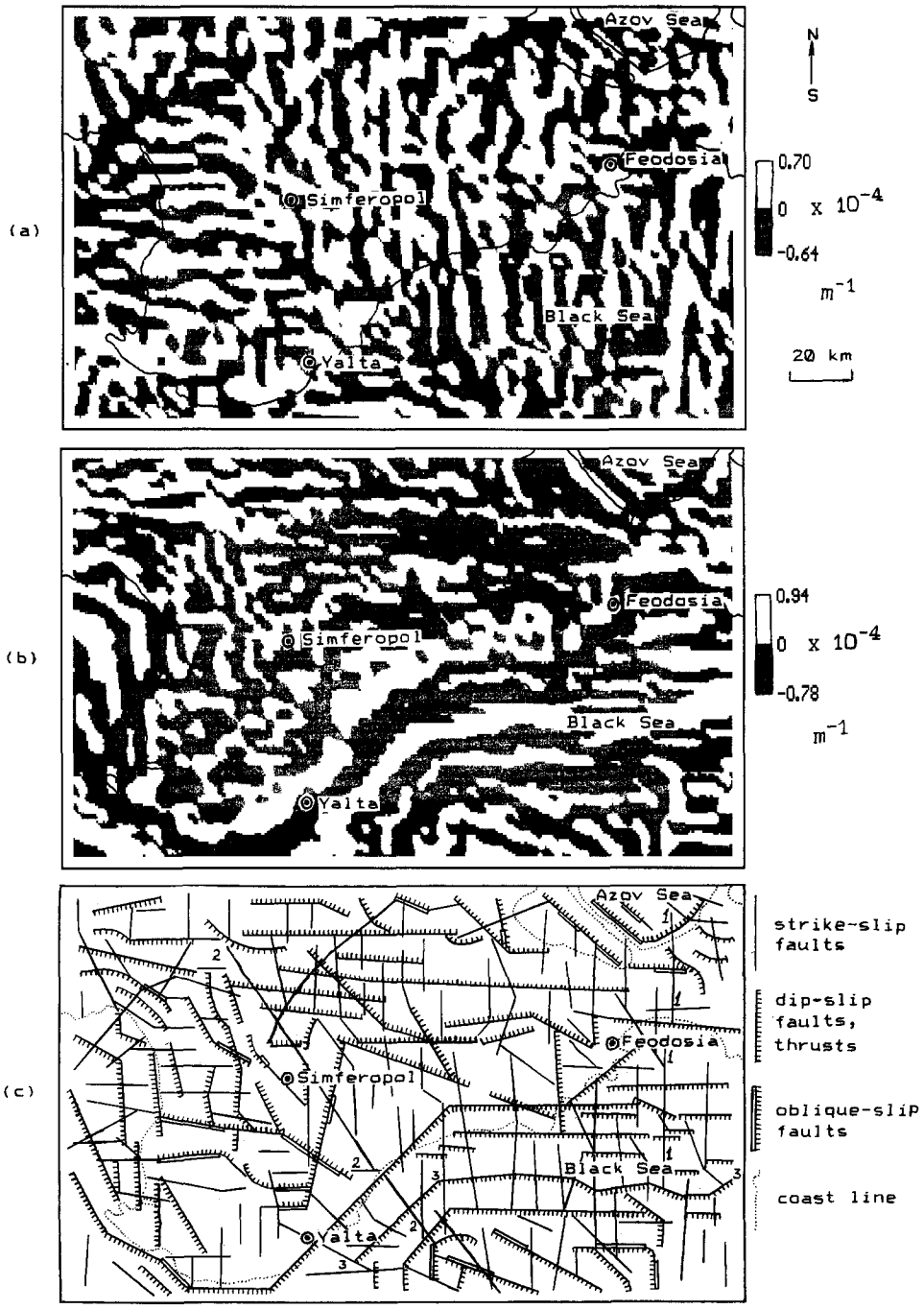

Fig. 5. The part of the Crimean Peninsula and the adjacent sea bottom: (a) the K_h map, (b) the K_v map, (c) the map of morphologically classified faults revealed by the K_h and K_v maps, *1-1* is the Korsak–Feodosia fault, *2–2* is the Simferopol–Alushta fault, *3–3* is the South Coast fault.

4.2.3. Geological and tectonic description

The following main tectonic elements can be distinguished within the study area: the Mountain Crimea meganticlinorium of the Mediterranean Alpine geosynclinal belt, two adjacent foredeeps and the Scythian Epipalaezoic plate (Fig. 4b) (Muratov, 1969; Beloussov and Volvovsky, 1989).

On land the meganticlinorium consists of the South Coast, the Kacha and the Tuak anticlinoria, the west Crimean, the east Crimean and the Sudak synclinoria, the northwest and the north limbs and the pericline. The anticlinoria comprise late Triassic and middle Jurassic schists, sandstones and terrigenous flyschs. There are middle Jurassic basic intrusive massifs within the South Coast anticlinorium. The South Coast and the Tuak anticlinoria have an imbricate structure. Synclinoria are formed by late Jurassic and early Cretaceous limestones, sandstones, conglomerates, flyschs and clays. The Jurassic volcanic massif is located within the east Crimean synclinorium. The northwest and the north limbs comprise late Cretaceous, Eocene and Neogene limestones, clays and marls. The pericline is mainly formed by Oligocene–Miocene marine clays and includes brachyanticlinal diapir folds and mud volcanoes. The south part of the meganticlinorium is located underwater of the Black Sea and comprises late Triassic, Jurassic and Cretaceous rocks.

The Indol-Kuban foredeep is predominantly formed by an Oligocene–Quaternary complex. The Sorokin foredeep comprises dislocated Paleocene–Eocene and Oligocene–Miocene complexes which are covered by Pliocene–Quaternary marine sediments.

There are the Alma depression, the Simferopol, the Novotsaritsino and the Novoselovskoye buried elevated blocks of the folded basement within the Scythian plate. Its basement is formed by Paleozoic schists, sandstones, limestones, basic and acid intrusive and effusive rocks. The sedimentary cover consists of early and middle Jurassic argillites, aleurolites and conglomerates, early Cretaceous terrigenous clays, sandstones and limestones, late Cretaceous carbonate rocks, Paleocene and Eocene clays and carbonate rocks, Oligocene, Miocene and Pliocene limestones, clays, marls and sandstones (Muratov, 1969; Beloussov and Volvovsky, 1989).

The study site is a tectonically active region, with many recorded seismic earthquakes foci (Muratov, 1969; Beloussov and Volvovsky, 1989; Borisenko, 1986).

The structure of the Crimean meganticlinorium and adjacent areas is complicated by a lot of faults (Fig. 4c). The following main fault groups can be distinguished (Muratov, 1937; Shalimov, 1966; Lvova, 1972; Rastsvetaev, 1977; Borisenko, 1986):

1. Near-north-striking left-lateral strike-slip faults with high-angle dips, 3–5 kilometer horizontal displacements and tens of kilometer lengths. They are most abundant in the eastern, central and southwestern parts of the study site.
2. Near-northeast and east-striking dip-slip faults with northwest dips and tens of metre displacements. Some researchers consider that these faults are thrusts with 30°–45° dips and several kilometres displacements.
3. Near-northwest-striking dip-slip and oblique-slip faults with high-angle dips. Oblique-slip faults have right-lateral 10–100 metres horizontal displacements.
4. Near-north-striking dip-slip faults located in the western part of the region.

4.2.4. Initial data and methods

To test the method the irregular DEM of the part of the Crimean Peninsula and the adjacent sea bottom was applied. This DEM was compiled by digitizing 1:300,000 and 1:500,000 scaled topographic maps (Florinsky, 1992). The irregular DEM includes 11,936 points. The regular DEM (Fig. 4a) was generated by the irregular DEM interpolation using the weighted average method (Schut, 1976). A matrix step of 500 m was used.

K_h and K_v digital models (Fig. 5a, b) were obtained by the algorithm of Evans (1980) using a matrix step of 3000 m. Utilization of this step allows us to believe that revealed lineaments have mostly tectonic origin.

The map of revealed and morphologically classified faults (Fig. 5c) was obtained by a visual analysis of the K_h and K_v maps (Fig. 5a, b). To estimate the efficiency of the method we carried out a visual comparative analysis of the fault map obtained (Fig. 5c) and some factual geological data (Moisejew, 1930, 1939; Muratov, 1937, 1969; Kovalevsky, 1965; Lebedev and Orovetsky, 1966; Shalimov, 1966;

Rozanov, 1970; Lvova, 1972; Rastsvetaev, 1977; Sollogub and Sollogub, 1977; Sidorenko, 1980; Kats et al., 1981; Abashin et al., 1982; Kozlovsky, 1984; Borisenko, 1986; Zaritsky, 1989).

We did not perform a strong correlation analysis of the fault map obtained (Fig. 5c) and published data, as the latter have dissimilar precision, scales, and are rather different from one another. For instance, some faults are revealed by all authors, others are included only into a certain map. Sometimes one and the same fault is presented with different lengths or strikes on different maps. At the same time, we cannot use a certain single published map because the cited data complement each other.

Interpolations of irregular DEMs, K_h and K_v calculation and mapping (Figs. 2, 4a, 5a, b) were realized by the software LANDLORD 2.0 (Florinsky et al., 1995) on an IBM PC AT 80286 computer.

5. Results and discussion

5.1. The imaginary area

Visual analysis of the maps obtained (Fig. 2) confirms that the theoretical basis of the method is mostly correct.

After dip-slip fault modeling (Fig. 2d, g) clear lineaments passing strictly along fault axes are recorded on K_v maps (Fig. 2f, i). Some vertical motion traces are also revealed by K_h mapping (Fig. 2e, h) but there are no lineaments along fault axes. The lineament corresponding to the vertical dip-slip fault (Fig. 2f) does not differ mainly from the lineament corresponding to the low-angle dip-slip fault (Fig. 2i).

After the strike-slip fault modeling (Fig. 2j) only K_h mapping allows us to reveal a small lineament in the lower part of the map (Fig. 2k). This lineament passes strictly along the dislocation axis. The K_v map does not contain lineaments (Fig. 2l) although strike-slip fault traces are revealed, which are a break of the valley and a displacement of its east part northward.

After the oblique-slip fault modeling (Fig. 2m) the clear expressed lineament, the break of the valley and the displacement of its eastern part northward are revealed on the K_v map (Fig. 2o). Vertical and horizontal motion traces are recorded by K_h mapping (Fig. 2n) but there is no theoretically presumed lineament along the fault axis. This fact contradicts the theoretical basis of the method and, in principle, can be connected with drawbacks of the oblique-slip fault modeling. Besides, we may probably suppose a lesser "sensitivity" of K_h to horizontal tectonic motions (Fig. 2k, n) as compared with K_v "sensitivity" to vertical movements (Fig. 2f, i, o). However, real DEMs processing demonstrates that both K_h and K_v mapping allow us to reveal lineaments with equal "sensitivity" level (Florinsky, 1992; Florinsky et al., 1995). Probably, this may be a result of erosion influence which can increase the topographic expression of faults, for instance, in forms of fault-line valleys or scarps. K_h and K_v equal "sensitivities" to horizontal and vertical tectonic motions correspondingly are demonstrated by testing the method with the use of the DEM of the Crimean Peninsula and the adjacent sea bottom (see below).

After thrust modeling (Fig. 2p, s) clear lineaments passing along fault axes are revealed by K_v mapping (Fig. 2r, u). Some overthrust traces are also recorded on K_h maps (Fig. 2q, t) but there are no lineaments along fault axes. The lineament of the overthrust with 5 m displacement (Fig. 2r) is thinner than the lineament of the overthrust with 15 m displacement (Fig. 2u). It is natural, because the thrust scarp in the second case (Fig. 2s) is larger than the thrust scarp in the first case (Fig. 2p). This results in greater variations of K_v values in the second case (Fig. 2u) than in the first case (Fig. 2r).

After the gaping fault modeling (Fig. 2v) the clear lineament is recorded on the K_h map (Fig. 2w) as well as the lineament broken by the valley is revealed by K_v mapping (Fig. 2x).

Modeled faults have constant displacements along their lines. It is doubtful if a non-constant offset may have any specific effect on K_h or K_v maps.

Apparently, if we change a strike of modeled faults we shall get fairly different K_h and K_v maps which, however, will not differ radically from the results obtained (Fig. 2).

Modeled faults are not distinctly recognized on elevation maps (Fig. 2d, g, j, m, p, s, v) because we deformed the initial DEM but not the initial elevation map (Fig. 2a) and used the contour interval 1 m.

Obviously, a DEM includes more elevation data than an elevation map compiled by the DEM processing. This fact emphasizes a need to use DEMs obtained by stereoplotter techniques.

To test the method we applied a very simple DEM and modeled single simple faults. Apparently, an unambiguous character and impartiality of fault revealing and morphology classification will decrease when we use complicated DEMs of real terrains.

5.2. *The part of the Crimean peninsula and the adjacent sea bottom*

K_h calculation and mapping allow us to reveal (a) a complex of near-north oriented lineaments in the east and central parts of the study site, (b) a complex of near-east oriented lineaments in the west part of the region, (c) some near-northeast oriented linear structures in the north part of the study site, and (d) some near-northwest oriented lineaments in the south part of the region (Fig. 5a). Lineaments revealed by K_h mapping correspond to convergence areas (K_h negative values) and are connected with a valley network. A strong dependence of the Crimean valley network on the regional fault network was noted even by Muratov (1937). Lineaments recorded on the K_h map (Fig. 5a) are mostly interpreted as strike-slip faults (Fig. 5c).

K_v calculation and mapping allow us to reveal (a) a complex of near-west oriented lineaments in the east and central part of the study site, (b) a complex of near-north oriented lineaments mainly in the west part of the region, and (c) some near-northwest oriented linear structures mostly in the south and the north part of the study site (Fig. 5b). Lineaments revealed by K_v mapping correspond to relative deceleration areas (K_v negative values) and are connected with terraces. These lineaments are mainly interpreted as dip-slip faults and thrusts (Fig. 5c).

Lineaments revealed on both K_h and K_v maps (Fig. 5a, b) are interpreted as oblique-slip faults (Fig. 5c).

The map of morphologically classified faults (Fig. 5c) displays a complicated spatial distribution of faults. Dip-slip, thrust and strike-slip faults unite, as a rule, into complexes. The complex of near-north-striking strike-slip faults stretches through areas of different geological origins which are the Scythian plate and the Mountain Crimea meganticlinorium. Dip-slip faults stretch, as a rule, across strike-slip faults. There are some complicated faults which include dip-slip, strike-slip, thrust and oblique-slip offsets stretching along the same fault line one after another (Fig. 5c). These tendencies of fault distribution were also found out by the method developed for the Kursk Region, Russia (Florinsky et al., 1995).

Obviously, the fault map obtained (Fig. 5 c) has a preliminary and somewhat subjective nature. First, it is a result of slightly ambiguous drawing of fault lines. As a rule, we drew median lines of lineaments recorded on the K_h and K_v maps (Fig. 5a, b). Second, a visual analysis of these maps may result in the loss of some lineaments. Probably, this problem can be solved by a pattern recognition method (Pratt, 1978). Third, the fault map (Fig. 5c) corresponds only to the single matrix step 3000 m. Using a smaller matrix step we can obtain a map which will include more faults, while using a larger step we will obtain a map with fewer faults.

A visual comparative analysis of the fault map obtained (Fig. 5c) and factual geological data (Moisejew, 1930, 1939; Muratov, 1937, 1969; Kovalevsky, 1965; Lebedev and Orovetsky, 1966; Shalimov, 1966; Rozanov, 1970; Lvova, 1972; Rastsvetaev, 1977; Sollogub and Sollogub, 1977; Sidorenko, 1980; Kats et al., 1981; Abashin et al., 1982; Kozlovsky, 1984; Borisenko, 1986; Zaritsky, 1989) made it apparent that a portion of revealed faults correlates with familiar ones. For instance, there are the Korsak–Feodosia, the Simferopol–Alushta and the South Coast faults (Figs. 4c, 5c). Another portion of revealed faults does not correlate with known structures. For the first time the complex of near-east-striking strike-slip faults is recognized in the western part of the region. Origin of these structures and their relationships with the regional tectonics is the subject of an individual study. It is very important that the most of the faults revealed and morphologically classified fit into the main regional fault groups (see above).

However, familiar faults were not all revealed. On the whole, this is the result of the use of the single matrix step. To recognize all the topographically expressed faults (and to range faults into trans-regional, regional and local groups) we have to use a

set of K_h and K_v maps correspond to several matrix steps or extents of DEM low-pass filtering and smoothing (Florinsky, 1992).

It is evident, that lineaments have different statistical properties (i.e., orientation, density, length) within different zones of the region (Fig. 5a, b). This phenomenon can be connected with different geological properties (rock age, mechanical characteristic, soils, water regime, etc.) of these zones (Stepanov, 1989; Kuryakova and Florinsky, 1991). Consequently, K_h and K_v data can be used for geological and soil regionalization and mapping. However, this problem lies beyond the subject of the present paper.

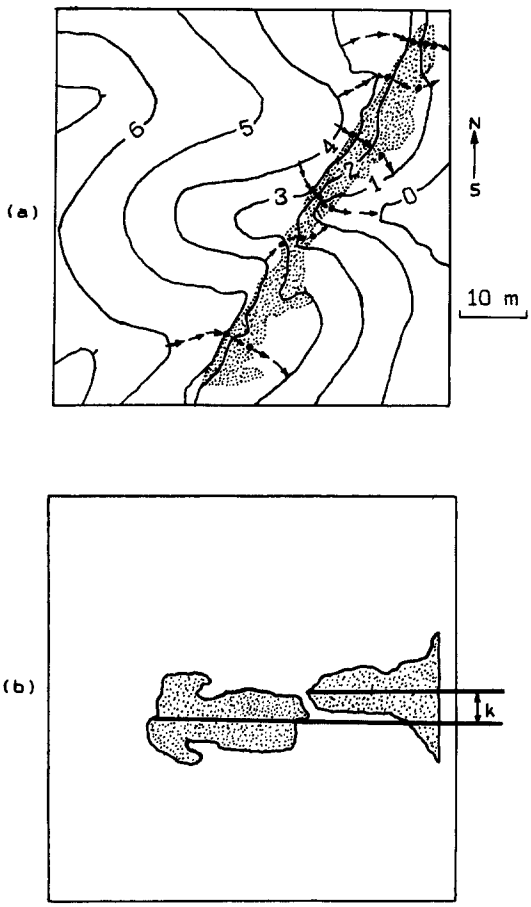

Fig. 6. Quantitative estimations of fault displacements: (a) the estimation of vertical displacement (Fig. 2d, f), the lineament is hachured, pointers are flow lines, big points are intersections of flow lines with the lineament; (b) the estimation of horizontal displacement (Fig. 2l), valley parts are hachured, k is the horizontal displacement.

The method developed can also be applied for the recognition of faults in specific stratigraphic horizons. The method has been used for mapping faults in the basement, Cenomanian and Cretaceous complex roofs of an area of the Kursk Nuclear Power-Station, Russia (Florinsky et al., 1995). Initial data were stratigraphic horizon DEMs. Maps of morphologically classified faults of different roofs were obtained. These maps essentially supplemented known geological data and can be applied to seismic regionalization and geological monitoring of the area. Obviously, fault recognition by stratigraphic DEMs processing is less impartial than with the use of landsurface DEMs.

The following question arises: is it possible to estimate quantitatively a fault displacement by a DEM analysis? For a simple surface with a single fault (Fig. 2) it can be realized easily. To determine the direction of a vertical displacement we have to compare elevations on one and the other sides of a lineament revealed on a K_v map. To estimate a vertical displacement we can use an average value of elevation amplitudes in points where flow lines (Young, 1972) intersect a lineament recorded on a K_v map (Fig. 6a). Obviously, the estimation precision depends on the erosion intensity, the DEM precision and resolution, and the number of measurements. A horizontal displacement of a strike-slip fault can be estimated by the analysis of relative displacements of valley parts recorded on a K_v map along a fault line (Fig. 6b). However, in studies of real territories with complicated topography and tectonic displacement estimations will also be complicated and subjective. Therefore, we did not estimate fault displacements for the Crimean Peninsula and the adjacent region.

The method requires further development. It is necessary to develop procedures for determination and separation of (a) tectonic and non-tectonic lineaments, (b) faults, folds and flexures, (c) dip-slip, reverse and thrust faults, and (d) oblique-slip and gaping faults. It is essential to improve the method impartiality. This can be realized by software consisting of (a) a geographical information system for DEMs, geological, geophysical and remotely sensed data processing and visualization, (b) a consulting expert system based on the knowledge of geological structure properties, and (c) a pattern recognition

module for automated revealing lineaments on K_h and K_v maps. The software can include other modules which may be of interest to the user (e.g., strike and dip measuring — Chorowicz et al., 1991; Morris, 1991).

6. Conclusions

For revealing and morphological recognition of topographically expressed faults it is necessary (a) to calculate K_h and K_v by a DEM processing (DEM resolution has to correspond to a typical size of faults under study), (b) to stratify K_h and K_v values into two levels with respect to the zero value, and (c) to map K_h and K_v. Lineaments revealed on K_h maps indicate faults formed mostly by horizontal tectonic motions (i.e., strike-slip faults). Lineaments recognized by K_v mapping correspond to faults formed mainly by vertical motions (i.e., dip-slip and reverse faults) and thrusting. Lineaments recorded on both K_h and K_v maps indicate, as a rule, oblique-slip and gaping faults.

The method was tested by processing the DEMs of an imaginary area with modeled faults and the DEM of the part of the Crimean Peninsula and the adjacent sea bottom. For the imaginary area the results obtained mostly correlate with the theoretical basis of the method. For the real area the comparative analysis of the results obtained and factual geological data demonstrates that the method actually works to identify individual faults in regions where both topography and tectonic structure are complicated.

The method developed is reproducible. It can improve information completeness and impartiality of laboratory geological work, contribute to their automation.

The method requires further development. Problems of the DEM precision as applied to fault recognition and the K_h and K_v calculation precision have to be investigated.

Acknowledgements

The author is grateful to Dr. P.A. Shary (Institute of Soil Science and Photosynthesis, Pushchino), Prof. V.G. Trifonov (Geological Institute, Moscow) for expert opinions, as well as to Dr. V.V. Bronguleev (Institute of Geography, Moscow) and two anonymous referees for useful criticism.

References

Abashin, A.A., Pasynkov, A.A. and Sidenko, O.G., 1982. Results of interpretation of space scenes of the Crimea. Tectonica i Stratigraphiya, 22: 35–39 (in Russian).

Bassett, K., 1972. Numerical methods for map analysis. In: C. Board, R.J. Chorley, P. Haggett and D.R. Stoddart (Editors), Progress in Geography. International Reviews of Current Research, Vol. 4, pp. 217–254.

Beloussov, V.V. and Volvovsky, B.S. (Editors), 1989. Structure and Evolution of the Earth Crust and Upper Mantle of the Black Sea. Nauka, Moscow, 207 pp. (in Russian, with English abstract and contents).

Borisenko, L.S., 1986. Geological criterion of seismic activity of the Crimea. Seismologicheskiye Issledovaniya, 9: 38–48 (in Russian, with English abstract).

Burdick, R.G. and Speirer, R.A., 1980. Development of a method to detect geologic faults and other linear features from Landsat images. Bureau of Mines, Report of Investigations, 8413: 1–74.

Campagna, D.J. and Levandowski, D.W., 1991. The recognition of strike-slip fault systems using imagery, gravity, and topographic data sets. Photogramm. Eng. Remote Sensing, 9: 1195–1201.

Carter, J.R., 1988. Digital representations of topographic surfaces. Photogramm. Eng. Remote Sensing, 11: 1577–1580.

Carter, J.R., 1992. The effect of data precision on the calculation of slope and aspect using gridded DEMs. Cartographica, 1: 22–34.

Chorowicz, J., Breard, J.Y., Guillande, R., Morasse, C.-R., Prudon, D. and Rudant, J.-P., 1991. Dip and strike measured systematically on digitized three-dimensional geological maps. Photogramm. Eng. Remote Sensing, 4: 431–436.

Clarke, K.C., 1988. Scale-based simulation of topographic relief. The American Cartographer, 2: 173–181.

Eliason, J.R. and Eliason, V.L.C., 1987. Process for structural geologic analysis of topography and point data. US Patent No. 4698759, International Classification G01V 3/18, US Classification 364/420, 107 pp.

Evans, I.S., 1980. An integrated system of terrain analysis and slope mapping. Z. Geomorphol. Suppl., 36: 274–295.

Florinsky, I.V., 1992. Recognition of Lineaments and Ring Structures: Quantitative Topographic Techniques. Pushchino Research Centre Press, Pushchino, 47 pp. (in Russian, with English abstract).

Florinsky, I.V., 1993. Digital Elevation Models Analysis for Linear Landsurface Structure Recognition. Ph.D. Thesis. Institute of Soil Science and Photosynthesis, Pushchino, 133 pp. (in Russian, unpubl.).

Florinsky, I.V., Grokhlina, T.I. and Mikhailova, N.I., 1995.

LANDLORD 2.0: the software for analysis and mapping of geometrical characteristics of relief. Geodesiya i Cartographiya, 5: 46–51 (in Russian).

Gzovsky, M.V., 1954. The main problems of fault classification. Sovetskaya Geologiya, 41: 131–169 (in Russian).

Hobbs, W.H., 1904. Lineaments of Atlantic Border region. Geol. Soc. Am. Bull., 15: 483–506.

Isaacson, D.L. and Ripple, W.J., 1990. Comparison of 7.5-minute and 1-degree digital elevation models. Photogramm. Eng. Remote Sensing, 11: 1523–1527.

Kats, Ja.G., Makarova, N.V., Kozlov, V.V. and Trofimov, D.M., 1981. Geological and geomorphological study of the Crimea by remotely sensed data interpretation. Izvestiya Vysshikh Uchebnykh Zavedeny, Geologiya i Razvedka, 3: 8–20 (in Russian).

Keller, E.A., 1986. Investigation of active tectonics: use of surficial earth processes. In: R.E. Wallace (Editor), Active Tectonics. National Academy Press, Washington, pp. 136–147.

Klinkenberg, B., 1992. Fractals and morphometric measures: is there a relationship? Geomorphology, 1/2: 5–20.

Korn, G.A. and Korn, T.M., 1968. Mathematical Handbook for Scientists and Engineers. Definitions, Theorems, and Formulas for Reference and Review. 2nd enl. and rev. ed. McGraw-Hill, New York, 1130 pp.

Kovalevsky, S.A., 1965. Median deep fault of the Crimean Peninsula. Doklady Academii Nauk SSSR, 4: 887–890 (in Russian).

Kozlovsky, E.A. (Editor), 1984. Space-Geological Map of the USSR, scale 1:2,500,000. Aerogeologiya, Moscow, 16 pp. (in Russian).

Kuryakova, G.A. and Florinsky, I.V., 1991. The Analysis of Space Relation between Ring Structures, Topography and Pedology. Pushchino Research Centre Press, Pushchino, 14 pp. (in Russian, with English abstract).

Lattman, L.H., 1958. Technique of mapping geologic fracture traces and lineaments on aerial photographs. Photogramm. Eng. Remote Sensing, 4: 568–576.

Lebedev, T.S. and Orovetsky, Yu.P., 1966. Peculiarities of the Mountain Crimea tectonics by new geological and geophysical data. Geophysichesky Sbornik, 18: 34–41 (in Russian).

Lvova, Ye.V., 1972. Neotectonic motions and formation of the Crimean coasts. In: I.I. Popov, Ye.M. Vasilenko and V.V. Nazin (Editors), Seismicity, Seismic Danger in the Crimea and Earthquake-Resistance of Building Trade. Naukova Dumka, Kiev, pp. 71–76 (in Russian).

Mandelbrot, B., 1967. How long is the coast of Britain? Statistical self-similarity and fractional dimension. Science, 3775: 636–638.

Masuoka, P.M., Harris, J., Lowman, P.D. Jr. and Blodget, H.W., 1988. Digital processing of orbital radar data to enhance geologic structure: examples from the Canadian Shield. Photogramm. Eng. Remote Sensing, 5: 621–632.

Moisejew, A.S., 1930. Geology of the South-West Part of the Main Ridge of the Crimean Mountains. Materialy po Obshchei i Prikladnoi Geologii, 89: pp. 1–82 (in Russian, with French abstract).

Moisejew, A.S., 1939. Essay of the tectonics of the North-Eastern Crimea. Uchenyye Zapiski Leningradskogo Universiteta, Seriya Geologo-Pochvennykh Nauk, 5: 155–189 (in Russian, with English abstract).

Moor, A.F. and Simpson, C.G., 1983. Image analysis — a new aid in morphotectonic studies. In: Proc. 17th Int. Symp. on Remote Sensing of Environment, Vol. 3. Environmental Research Institute of Michigan, Ann Arbor, pp. 991–1002.

Morris, K., 1991. Using knowledge-base rules to map the three-dimensional nature of geological features. Photogramm. Eng. Remote Sensing, 9: 1209–1216.

Muratov, M.V., 1937. Geological description of the east part of the Crimean Mountains. Trudy Moscowskogo Geologo-Razvedochnogo Instituta, 7: 21–122 (in Russian).

Muratov, M.V. (Editor), 1969. Geology of the USSR. Vol. 8. The Crimea. Part 1. Geological Description. Nedra, Moscow, 575 pp. (in Russian).

Nezametdinova, S.S., 1970. Analysis of Regional Fault Strikes within Oil- and Gas-Bearing Areas (Examples from the Precaucasus). Ph.D. Thesis Abstract. Leningrad Mining Institute, Leningrad, 17 pp. (in Russian).

Ollier, C., 1981. Tectonics and Landforms. Longman, London, 324 pp.

Onorati, G., Poscolieri, M., Salvi, S. and Trigila, R., 1987. Use of TM Landsat data as a support to classical ground-based methodologies in the investigation of a volcanic site in Central Italy the Caldera of Latera. In: IGARSS'87. Remote Sensing: Understanding the Earth as a System. Proc. IEEE Int. Geoscience and Remote Sensing Symp., Ann Arbor, 18–21 May, 1987. Vol. 2. IEEE, New York, pp. 1173–1178.

Onorati, G., Poscolieri, M., Ventura, R., Chiarini, V. and Crucilla, U., 1992. The digital elevation model of Italy for geomorphology and structural geology. Catena, 2: 147–178.

Peive, A.V., 1956. General characteristics, classification and spatial distribution of deep faults. 1. The main types of deep faults. Izvestiya Academii Nauk SSSR, Seriya Geologicheskaya, 1: 90–105 (in Russian).

Phylosophov, V.P., 1960. Brief Manual on the Morphometric Method for Tectonic Structure Search. Saratov University Press, Saratov, 94 pp. (in Russian).

Pratt, W.K., 1978. Digital Image Processing. Wiley, New York, 750 pp.

Rastsvetaev, L.M., 1977. The Mountain Crimea and the North Black Sea area. In: A.I. Suvorov (Editor), Faults and Horizontal Movements of Mountain Chain of the USSR. Nauka, Moscow, pp. 95–113 (in Russian).

Rozanov, L.N. (Editor), 1970. Tectonic map of oil- and gas-bearing regions of the USSR, scale 1:2,500,000. All-Union Air-Geological Trust, Moscow, 16 pp. (in Russian).

Schowengerdt, R.A. and Glass, C.E., 1983. Digitally processed topographic data for regional tectonic evaluations. Geol. Soc. Am. Bull., 4: 549–556.

Schut, G.H., 1976. Review of interpolation methods for digital terrain models. The Canadian Surveyor, 5: 389–412.

Shalimov, A.I., 1966. A new tectonic scheme of the Crimea and the connection between fold structures of the Mountain Crimea and the North-West Caucasus. In: V.A. Magnitsky, Yu.D.

Bulange and Yu.A. Meshcheryakov (Editors), The Structure of the Black Sea Depression. Nedra, Moscow, pp. 49–58 (in Russian, with English abstract).

Shary, P.A., 1991. The second derivative topographic method. In: I.N. Stepanov (Editor), The Geometry of the Earth Surface Structures. Pushchino Research Centre Press, Pushchino, pp. 30–60 (in Russian).

Sidorenko, A.V. (Editor), 1980. Map of Faults of the USSR and Territories of Adjacent States, scale 1:2,500,000. Aerogeologiya, Moscow, 20 pp. (in Russian).

Slemmons, D.B. and Depolo, C.M., 1986. Evaluation of active faulting and associated hazards. In: R.E. Wallace (Editor), Active Tectonics. National Academy Press, Washington, pp. 45–62.

Sollogub, V.B. and Sollogub, N.V., 1977. Structure of the Earth Crust of the Crimean Peninsula. Sovetskaya Geologiya, 3: 85–93 (in Russian).

Stepanov, I.N. (Editor), 1989. Map of Landsurface Systems and Soil Cover of the Part of the Middle Asia, scale 1:1,500,000. The Central Board of Geodesy and Cartography of the Council of Ministers of the USSR, Moscow, 2 pp. (in Russian).

Thienssen, R.L., Soofi, K. and Sheline, H., 1994. A new expandable detector applied to digital topography and TM image data in support of petroleum exploration. Photogramm. Eng. Remote Sensing, 1: 77–85.

Trifonov, V.G., 1983. Late Quaternary Tectonics. Nauka, Moscow, 224 pp. (in Russian, with English contents).

Trifonov, V.G., Makarov, V.I., Safonov, Yu.G. and Florensky, P.V. (Editors), 1983. Space Information for Geology. Nauka, Moscow, 535 pp. (in Russian, with English contents).

Ulyanov, P.A., 1977. Gibbs phenomenon. In: I.M. Vinogradov (Editor), Mathematical Encyclopaedia, Vol. 1. Soviet Encyclopaedia Press, Moscow, pp. 958–959 (in Russian).

Vinogradova, A.I. and Yeremin, V.K. (Editors), 1971. Air Methods for Geological Investigations. Nedra, Leningrad, 703 pp. (in Russian).

Wallace R.E., 1986. Overview and recommendations. In: R.E. Wallace (Editor), Active Tectonics. National Academy Press, Washington, pp. 3–19.

Wilson, J.T., 1941. Structural features in the Northwest Territories. Am. J. Sci., 7: 493–502.

Wise, D.U., 1969. Regional and sub-continental sized fracture systems detectable by topographic shadow techniques. Can. Geol. Surv. Pap., 68-52, 175–198.

Young, A., 1972. Slopes. Oliver and Boyd, Edinburgh, 288 pp.

Zaritsky, A.I. (Editor), 1989. Map of Linear and Ring Structures of the Ukrainian Soviet Socialist Republic (by Remotely Sensed Data), scale 1:1,000,000. Ukrgeologiya, Kiev, 4 pp. (in Russian).

Zlatopolsky, A.A., 1988. The software for recognition and analysis of linear elements on remotely sensed images. In: B.N. Mozhaev (Editor), Automated Analysis of Natural Lineament Systems. All-Union Scientific Research Geological Institute, Leningrad, pp. 14–28 (in Russian).